JCI insight

Chronic-plus-binge alcohol intake induces production of proinflammatory mtDNA-enriched extracellular vesicles and steatohepatitis via ASK1/p38MAPKα-dependent mechanisms

Jing Ma, … , Jian Sun, Bin Gao

JCI Insight. 2020;5(14):e136496. https://doi.org/10.1172/jci.insight.136496.

Research Article Hepatology

Graphical abstract

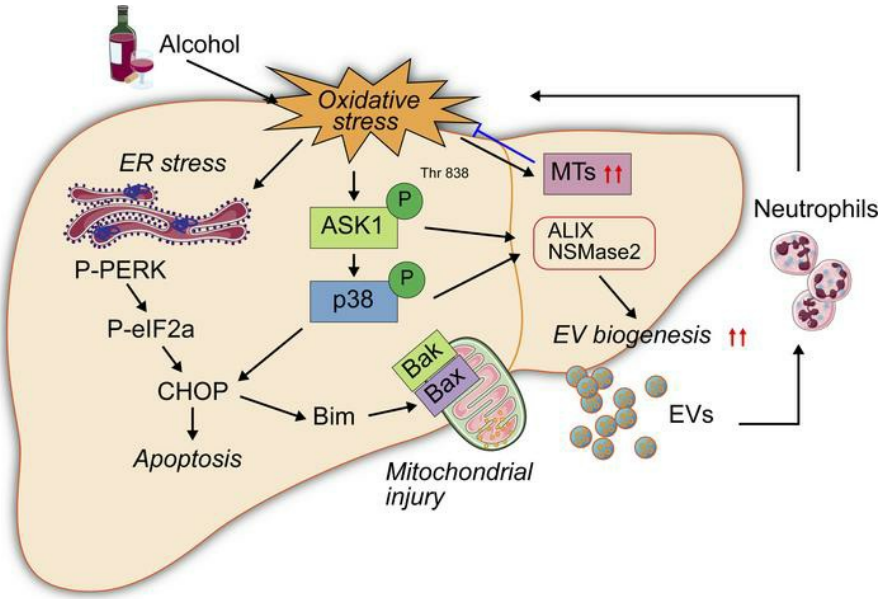

JCI insight

RESEARCH ARTICLE

Chronic-plus-binge alcohol intake induces production of proinflammatory mtDNA-enriched extracellular vesicles and steatohepatitis via ASK1/p38MAPKα-dependent mechanisms

Jing Ma,[1,2] Haixia Cao,[2] Robim M. Rodrigues,[2] Mingjiang Xu,[2] Tianyi Ren,[2] Yong He,[2] Seonghwan Hwang,[2] Dechun Feng,[2] Ruixue Ren,[2] Peixin Yang,[3] Suthat Liangpunsakul,[4,5,6] Jian Sun,[1] and Bin Gao[2]

[1]State Key Laboratory of Organ Failure Research, Department of Infectious Diseases, Nanfang Hospital, Southern Medical University, Guangzhou, China. [2]Laboratory of Liver Diseases, National Institute on Alcohol Abuse and Alcoholism, NIH, Bethesda, Maryland, USA. [3]Department of Obstetrics and Gynecology Science, University of Maryland, School of Medicine, Baltimore, Maryland, USA. [4]Division of Gastroenterology and Hepatology, Department of Medicine, and [5]Department of Biochemistry and Molecular Biology, Indiana University School of Medicine, Indianapolis, Indiana, USA. [6]Roudebush Veterans Administration Medical Center, Indianapolis, Indiana, USA.

Alcohol-associated liver disease is a spectrum of liver disorders with histopathological changes ranging from simple steatosis to steatohepatitis, cirrhosis, and hepatocellular carcinoma. Recent data suggest that chronic-plus-binge ethanol intake induces steatohepatitis by promoting release by hepatocytes of proinflammatory mitochondrial DNA–enriched (mtDNA-enriched) extracellular vesicles (EVs). The aim of the present study was to investigate the role of the stress kinase apoptosis signal–regulating kinase 1 (ASK1) and p38 mitogen-activated protein kinase (p38) in chronic-plus-binge ethanol–induced steatohepatitis and mtDNA-enriched EV release. Microarray analysis revealed the greatest hepatic upregulation of metallothionein 1 and 2 (*Mt1/2*), which encode 2 of the most potent antioxidant proteins. Genetic deletion of the *Mt1* and *Mt2* genes aggravated ethanol-induced liver injury, as evidenced by elevation of serum ALT, neutrophil infiltration, oxidative stress, and ASK1/p38 activation in the liver. Inhibition or genetic deletion of *Ask1* or *p38* ameliorated ethanol-induced liver injury, inflammation, ROS levels, and expression of phagocytic oxidase and ER stress markers in the liver. In addition, inhibition of ASK1 or p38 also attenuated ethanol-induced mtDNA-enriched EV secretion from hepatocytes. Taken together, these findings indicate that induction of hepatic mtDNA-enriched EVs by ethanol is dependent on ASK1 and p38, thereby promoting alcoholic steatohepatitis.

Authorship note: JM and HC contributed equally to this work and share first authorship.

Conflict of interest: The authors have declared that no conflict of interest exists.

Submitted: January 16, 2020
Accepted: June 5, 2020
Published: July 23, 2020.

Reference information: *JCI Insight*. 2020;5(14):e136496. https://doi.org/10.1172/jci.insight.136496.

Introduction

Alcohol-associated liver disease (ALD) is the leading cause of liver-related morbidity and mortality worldwide, contributing to approximately half of liver cirrhosis cases in Western countries (1–3). ALD encompasses a broad spectrum of hepatic pathologies, ranging from simple steatosis to severe forms of liver injury such as alcoholic steatohepatitis, progressive fibrosis, end-stage cirrhosis, complications from portal hypertension, and superimposed hepatocellular carcinoma (HCC) (1–3). The short-term mortality of patients with severe alcoholic hepatitis is very high (20%–50% at 3 months) (2). Although significant scientific progress has been made in understanding the disease process, the pathogenesis of ALD remains elusive, with significant impact on the discovery of mechanism-based therapies (1–3). The development of such therapies requires translational studies using human samples and suitable animal models that reproduce clinical and histological features of alcoholic hepatitis. One of the major advances in the field of ALD research was the introduction of binge ethanol in chronically ethanol-fed mice (4, 5), which causes neutrophilia and hepatic neutrophil infiltration, simulating some features of

human alcoholic hepatitis. By use of this chronic-plus-binge ethanol feeding model, many novel mechanisms underlying ALD have been identified (6, 7). For example, we have recently demonstrated that binge ethanol intake activates liver mitochondrial DNA–enriched (mtDNA-enriched) extracellular vesicle (EV) release in chronically ethanol-fed mice and in patients with alcohol use disorder, leading to neutrophilia and liver injury (8). However, the molecular mechanisms by which binge ethanol intake induces hepatic mtDNA-enriched EV release remain unknown.

Previous studies have identified several mechanisms involved in the pathogeneses of ALD, including ethanol metabolism–associated oxidative stress, glutathione depletion, abnormal methionine metabolism secondary to malnutrition, ethanol-mediated induction of endotoxins from the impairment of intestinal permeability and subsequent activation of Kupffer cells (9–12). Oxidative stress is driven by molecules such as ROS and reactive nitrogen species (RNS), formed during ethanol metabolism, which can lead to activation of MAPKs. Yet the mechanisms by which ROS activates these kinases are unclear. It has been reported that ROS can activate MAPK pathways via the activation of growth factor receptors in several cell types (13) or via the oxidative modification of intracellular kinases (e.g., MAPK kinase kinase [MAP3K]) that are involved in MAPK signaling cascade (14). Another potential mechanism for MAPK activation by ROS may include the inactivation and degradation of the MAPKs that maintain the pathway in an inactive state (15). Activation of MAPKs, which are involved in the transduction of most extracellular signals, is one of the major signal transduction mechanisms by which the cell adapts to changes in the surrounding environment (e.g., oxidative stress, ER stress, calcium overload, ATP, Fas ligand, as well as inflammatory signals such as TNF and LPS) (16). The apoptosis signal–regulating kinase 1 (ASK1)/p38 MAPK (p38) signaling pathway is one of the major stress MAPKs that mediates diverse biological signals leading to cell death, differentiation, survival, and senescence as a response to cellular stress factors (16). The ASK1/p38 pathway has been described in *C. elegans* as a defense mechanism against bacterial attack, suggesting that this MAPK signaling cassette represents an ancient, evolutionarily conserved component in innate immunity (17). There are 4 isoforms (α, β, γ, and δ) of p38 MAPKs; however, the α-isoform has been postulated to be the most important in inflammation (18). Most of the studies have focused on p38α and identified an important function of p38α in tissue homoeostasis and pathologies from inflammation to cancer, heart, neurodegenerative diseases and metabolic syndrome, making p38α an interesting pharmaceutical target (19–21).

Multiple studies have demonstrated that the activation of hepatic ASK1/p38 signaling pathways contributes to regulation of hepatic lipid metabolism, inflammation, fibrosis, and systemic insulin resistance in mice (22–26). However, how the ASK1/p38 signaling pathway contributes to liver inflammation remains largely unknown. In this study, we provide evidence that the ASK1/p38 pathway, which is regulated by the antioxidant protein metallothionein (MT), plays an important role in controlling hepatic mtDNA-enriched EV release in chronic-plus-binge ethanol–fed mice, thereby promoting liver inflammation and injury.

Results

Hepatic Mt1/2 expression is highly elevated in chronic-plus-binge ethanol–fed mice, playing an important role in ameliorating ALD. Oxidative stress is a prominent mediator of alcoholic hepatitis (1). To investigate the regulation of oxidative stress–associated genes after chronic-plus-binge ethanol feeding, microarray analyses of liver samples from mice fed ethanol for 8 weeks (E8w) and mice fed ethanol for 8 weeks plus 1 binge (E8w+1B) were performed as previously described (27). Microarray analysis revealed a significant modulation of 46 oxidative stress–associated genes in E8w+1B mice compared with E8w mice. Among the most highly upregulated genes, *Mt1* and *Mt2* were elevated by 33-fold and 20-fold, respectively (Figure 1A). This result was further confirmed by reverse transcription quantitative PCR (RT-qPCR), showing *Mt1* and *Mt2* upregulation of 60-fold and 40-fold in E8w+1B mice compared with E8w mice, respectively. No modulation in *Mt1* and *Mt2* expression was found between pair-fed and E8w mice (Figure 1B). In addition, RT-qPCR analysis demonstrated that hepatic expression of *Mt1* and *Mt2* was upregulated 6-fold after a single ethanol binge alone (Supplemental Figure 1A; supplemental material available online with this article; https://doi.org/10.1172/jci.insight.136496DS1). Hepatic expression of *Mt1* and *Mt2* was also markedly upregulated in short-term chronic plus 1 binge (E10d+1B) compared with pair-fed mice (Figure 1B). Elevated hepatic expression of *Mt1* and *Mt2* was also observed in mice fed high-fat diet (HFD) or chow plus 1 binge, and their expression was significantly greater in the HFD+1B group (Supplemental Figure 1B). Interestingly, a significant induction of expression of *Mt1* and *Mt2* after 1 binge was only observed in the liver and not in kidney, heart, spleen, or pancreas (Supplemental Figure 1C).

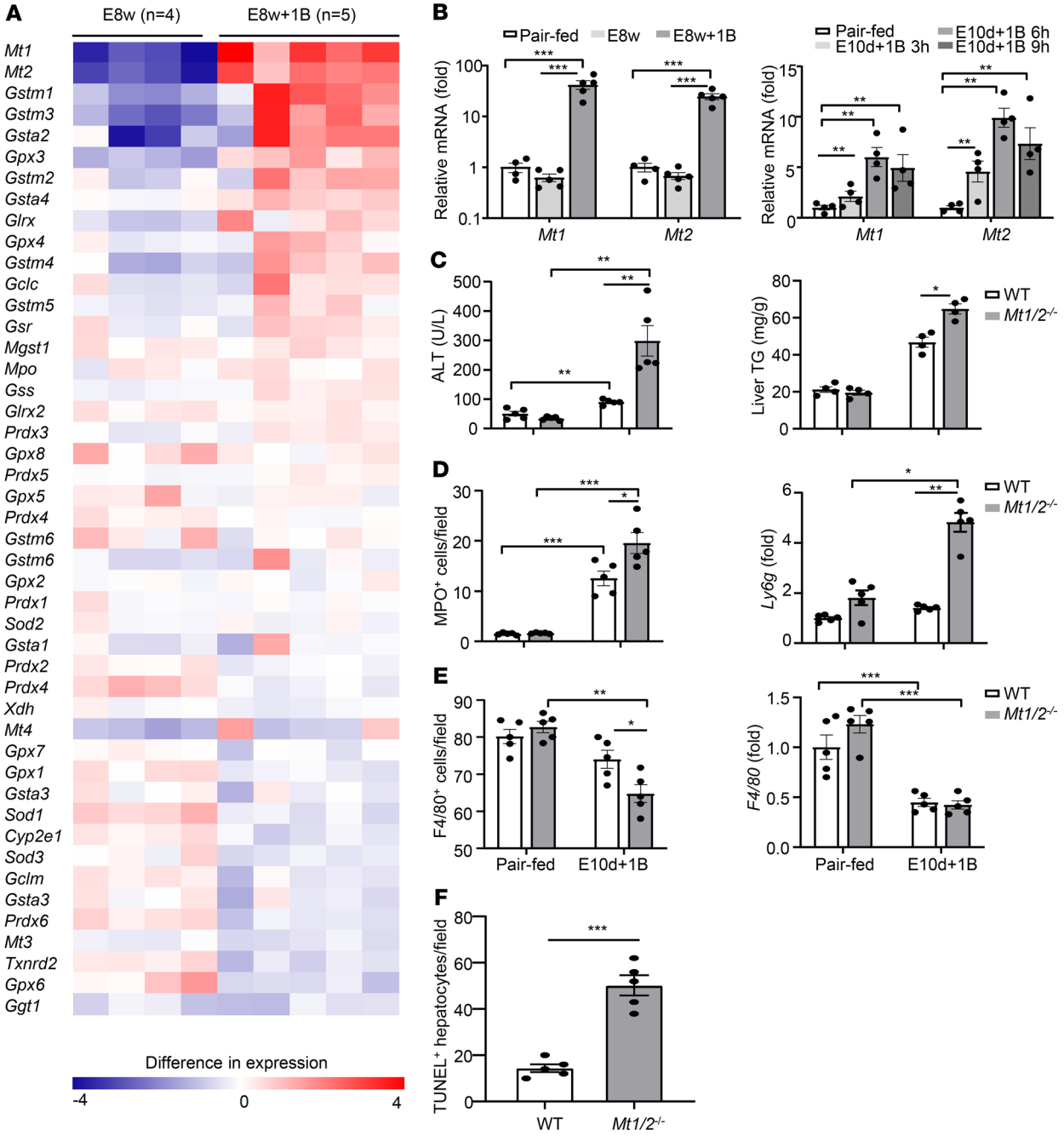

Figure 1. *Mt1/2*$^{-/-}$ mice are more susceptible to chronic-plus-binge ethanol–induced liver injury. (**A**) C57BL/6N mice were fed an ethanol diet for 8 weeks (E8w) or 8 weeks plus 1 binge (E8w+1B). Liver tissues were collected 9 hours after binge in the E8w+1B group and subjected to microarray analysis. A heat map of oxidative stress–related genes is shown. (**B**) C57BL/6N mice were pair-fed with control diet (pair-fed, $n = 4$) or fed an ethanol diet for 8 weeks (E8w), or E8w+1B, and were euthanized 9 hours after binge. C57BL/6N mice were fed a control diet (pair-fed) or ethanol diet for 10 days plus 1 binge (E10d+1B) and were euthanized 3, 6, or 9 hours later. Hepatic mRNA levels of *Mt1* and *Mt2* were examined by RT-qPCR. (**C**–**F**) WT and *Mt1/2*$^{-/-}$ mice were pair-fed or fed an ethanol diet for 10 days, followed by gavage of a single dose of maltose or ethanol, respectively and were euthanized 9 hours later. Serum ALT levels and hepatic TG levels were measured (**C**). Hepatic neutrophils were examined by IHC staining with an anti-MPO antibody or RT-qPCR analysis of *Ly6g* mRNA (**D**). Hepatic macrophages were examined by immunostaining with an anti-F4/80 antibody or RT-qPCR analysis of *F4/80* mRNA (**E**). Liver tissues were also subjected to TUNEL staining, and the TUNEL^{+} hepatocytes were counted (**F**). Values represent mean ± SEM (each dot represents 1 mouse sample). Statistical evaluation was performed by Student's *t* test or 1-way ANOVA with Tukey's post hoc test for multiple comparisons. $^{*}P < 0.05$, $^{**}P < 0.01$, $^{***}P < 0.001$.

To determine the role of MT1/2 in ALD, we subjected *Mt1/2*$^{-/-}$ and corresponding WT mice to chronic-plus-binge feeding. As illustrated in Figure 1C, *Mt1/2*$^{-/-}$ mice had higher levels of serum ALT and a higher degree of hepatic steatosis as indicated by hepatic triglyceride levels compared with WT mice. Hepatic neutrophils were examined by IHC and RT-qPCR analysis. As showed in Figure 1D and

Supplemental Figure 2, the number of myeloperoxidase-positive (MPO-positive) neutrophils in the liver was elevated in both WT and *Mt1/2*$^{-/-}$ mice after chronic-plus-binge feeding, with a higher number in *Mt1/2*$^{-/-}$ mice. Hepatic expression of *Ly6g* was also significantly increased after ethanol feeding of *Mt1/2*$^{-/-}$ mice but not WT mice. Interestingly, the number of F4/80^{+} macrophages and hepatic expression of *F4/80* were decreased in both WT and *Mt1/2*$^{-/-}$ mice after chronic-plus-binge feeding (Figure 1E and Supplemental Figure 2). Finally, the number of apoptotic TUNEL^{+} hepatocytes was higher in ethanol-fed *Mt1/2*$^{-/-}$ compared with WT mice (Figure 1F).

Deletion of Mt1/2 exacerbates oxidative stress and activation of stress kinases in ethanol-fed mice. To examine the role of MT1/2 in the control of oxidative stress and its associated kinase activation, we first measured hepatic levels of lipid peroxides including 4-hydroxynonenal (4-HNE) and malonaldehyde (MDA) and activated ASK1 and p38 MAPK in ethanol-fed and pair-fed mice. As shown in Supplemental Figure 3A, hepatic expression of 4-HNE and MDA was higher in mice subjected to E10d+1B treatment than in pair-fed mice. ASK1 is a MAPK that mediates ROS-induced cell death through activation of stress kinases such as p38 MAPK and JNK (28, 29). To understand whether MAPK signal is activated in ALD, we performed immunostaining of p-ASK1 and p-p38 in ethanol- and pair-fed mice. As shown in Supplemental Figure 3B, higher levels of hepatic pASK1 (Thr838) and p-p38 expression were observed in ethanol-fed compared with pair-fed mice.

To further confirm the role of MT1/2 in the activation of MAPK induced by oxidative stress in ALD, we examined hepatic oxidative stress and MAPK activation in ethanol-fed *Mt1/2*$^{-/-}$ and WT mice. Hepatic levels of 4-HNE and MDA were higher in ethanol-fed *Mt1/2*$^{-/-}$ mice than in ethanol-fed WT mice, as illustrated by Western blot analysis (Figure 2A) and thiobarbituric acid–reactive substance (TBARS) assays (Figure 2B). Higher levels of hepatic MDA and 4-HNE in ethanol-fed *Mt1/2*$^{-/-}$ versus WT mice were also evidenced by IHC staining analyses (Figure 2C). Correspondingly, stronger phosphorylation of ASK1 and p38 was detected in ethanol-fed *Mt1/2*$^{-/-}$ mice than in WT mice (Figure 2D).

Deletion of the Ask1 gene or administration of ASK1 inhibitors ameliorates ALD in mice. To further confirm the role of ASK1 in ALD, we performed chronic-plus-binge ethanol feeding (E10d+1B) of WT and *Ask1*$^{-/-}$ mice. First, downstream signaling of ASK1 pathway was examined by Western blot analysis. As shown in Supplemental Figure 4A, activation of hepatic p38 and JNK1/2 was dramatically lower in *Ask1*$^{-/-}$ versus WT mice after E10d+1B treatment. In contrast, activation of hepatic STAT3 was higher in *Ask1*$^{-/-}$ mice compared with WT controls.

Serum levels of ALT were lower in ethanol-fed *Ask1*$^{-/-}$ mice than in WT mice, as was the percentage of circulating neutrophils (Figure 3A). Absolute neutrophil counts in the peripheral blood were also decreased; however, this difference was not statistically significant (Supplemental Figure 4B). In addition, compared with ethanol-fed WT mice, ethanol-fed *Ask1*$^{-/-}$ mice showed a lower number of MPO^{+} neutrophils and F4/80^{+} macrophages, and lower expression of hepatic *Ly6g* and *F4/80* and several other inflammatory mediators (Supplemental Figure 4, C and D). Moreover, hepatic levels of 4-HNE and MDA (Figure 3B), as well as expression of phagocytic oxidase units, including *p47*^{phox}, *p22*^{phox}, *p40*^{phox}, and *gp91*^{phox} (Supplemental Figure 4E), were lower in ethanol-fed *Ask1*$^{-/-}$ mice than in WT mice. In addition, hepatic expression of several ER stress–associated genes, including *Ero1a*, *Ero1b*, *Bim*, *Gadd34*, *Pdi*, *Bax*, and *Bak*, were also markedly lower in *Ask1*$^{-/-}$ compared with WT mice after E10d+1B treatment (Supplemental Figure 4F). Finally, a decreased number of apoptotic TUNEL^{+} hepatocytes was detected in ethanol-fed *Ask1*$^{-/-}$ mice compared with WT mice (Supplemental Figure 4G).

Further evaluation on the role of ASK1 in ALD was conducted using a pharmacological approach by treating chronic-plus-binge ethanol–fed mice with 2 ASK1 inhibitors (NQDI-1 and GS-4997). As shown in Supplemental Figure 5A, hepatic activation of ASK1 and p38, as measured by their phosphorylated forms, was strongly attenuated after treatment with these 2 inhibitors, with stronger inhibition by GS-4997. Treatment with NQDI-1 or GS-4997 ameliorated hepatic injury, as demonstrated by a significant reduction in serum ALT without an affect on the percentage or absolute count of circulating neutrophils (Figure 4A). The numbers of MPO^{+} neutrophils and F4/80^{+} macrophages in the liver were lower in ethanol-fed mice treated with NQDI-1 or GS-4997 compared with those treated with vehicle (Figure 4B). Hepatic expression of *F4/80* mRNA but not *Ly6g* was lower in mice treated with ASK1 inhibitors compared with those with treated with vehicle (Figure 4B). Moreover, treatment with ASK1 inhibitors also reduced hepatic expression of some inflammatory mediators (e.g., *Tnfa*, *Vcam1*, and *Mip1a*) (Supplemental Figure 5B).

ASK1 inhibitor treatment also ameliorated hepatic levels of 4-HNE and MDA (Figure 5A). To understand the mechanism underlying the effects of ASK1 inhibitors on oxidative stress, we examined hepatic

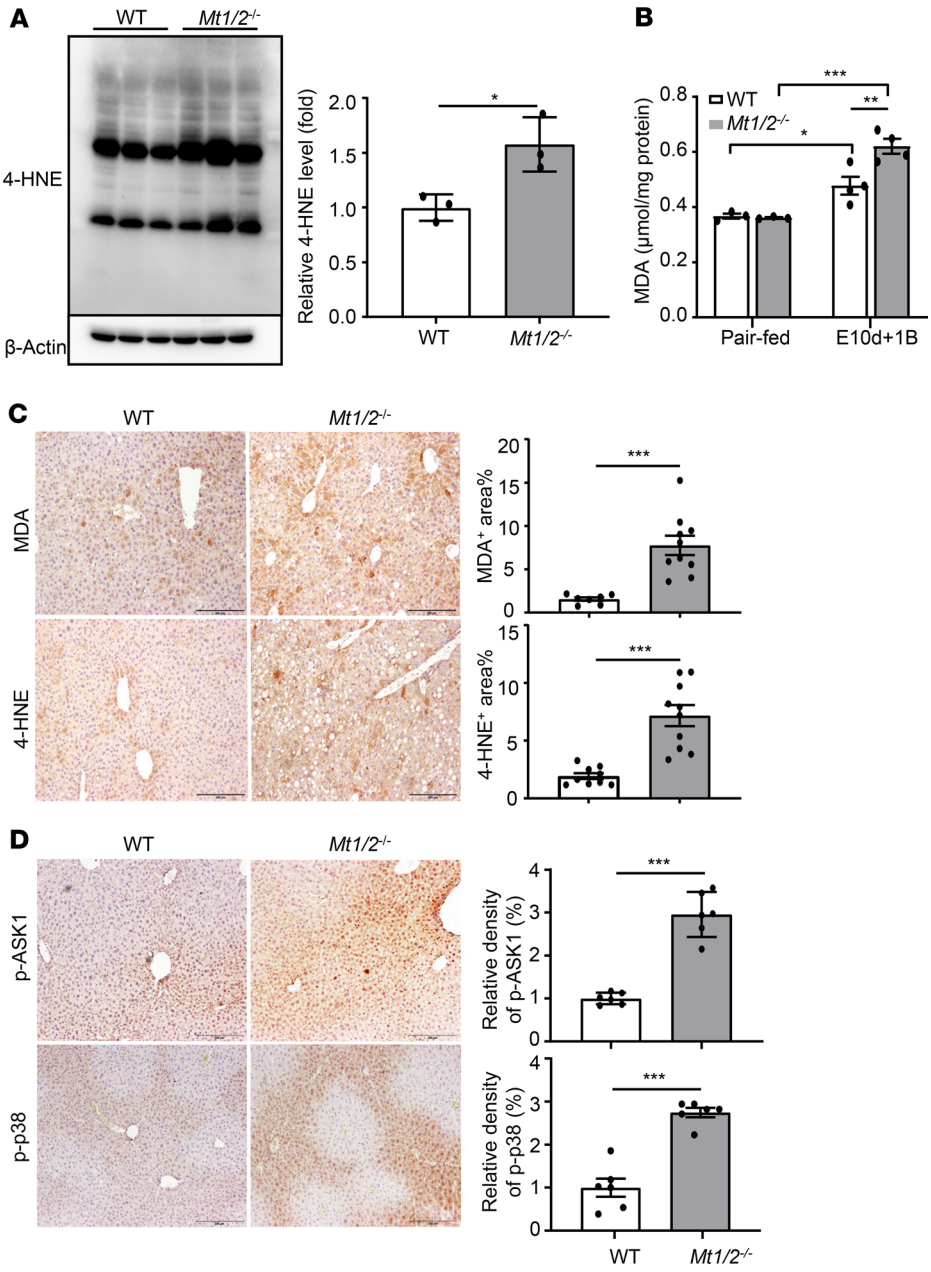

Figure 2. Deletion of the *Mt1/2* gene enhances oxidative stress and ASK1/p38 MAPK activation in the E10d+1B model. WT and *Mt1/2*$^{-/-}$ mice were fed an ethanol-containing diet for 10 days, followed by gavage of ethanol, and were euthanized 9 hours later. (**A**) Liver tissues from ethanol-fed mice were subjected to immunoblot analysis of 4-HNE. Quantification of 4-HNE was normalized to β-actin. (**B**) Liver tissues were subjected to TBARS assay for determination of MDA levels. (**C**) Liver tissues were subjected to IHC staining with antibodies against MDA and 4-HNE. Representative images (scale bars: 100 μm) and quantification of the area positive for each staining are shown. (**D**) Liver tissues were subjected to immunostaining with antibody against p-ASK1 or p-p38. Representative images (scale bars: 200 μm) and quantification of the positive area or density for each staining are shown. Values represent mean ± SEM (each dot represents 1 mouse sample). Statistical evaluation was performed by Student's *t* test or 1-way ANOVA with Tukey's post hoc test for multiple comparisons. *$P < 0.05$, **$P < 0.01$, ***$P < 0.001$.

expression of NADPH-associated molecules. Five phagocytic oxidase (phox) units — *p47*^{phox}, *p67*^{phox}, *p40*^{phox}, *gp91*^{phox}, and *p22*^{phox} — were found to be downregulated after treatment with ASK1 inhibitors (Supplemental Figure 5C). Next, we examined hepatic ER stress by detecting hepatic expression of ER stress–associated genes and proteins. RT-qPCR revealed that hepatic expression of *Ero1a*, *Ero1b*, *Gadd34*, *Pdi*, *Bax*, and *Bak* was significantly decreased after treatment with ASK1 inhibitors (Supplemental Figure 5D). Western blot analysis also showed downregulation of several ER stress–related proteins (i.e., CHOP, p-JNK1/2) after

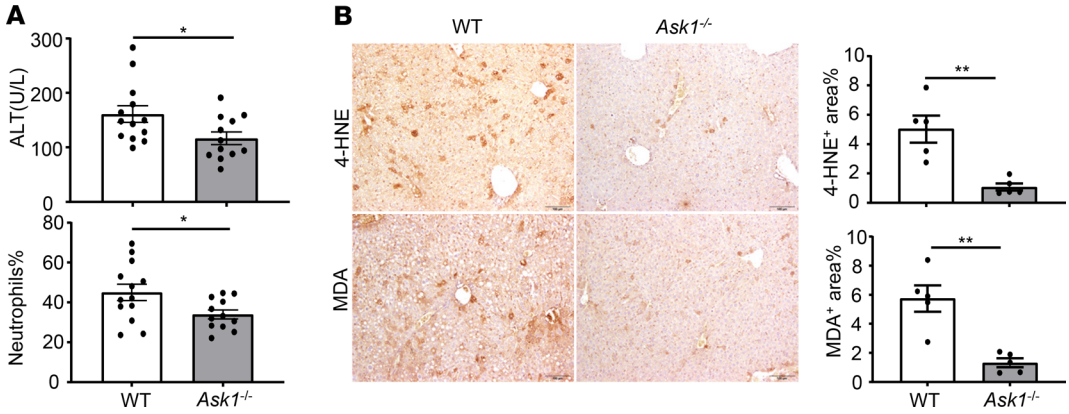

Figure 3. Deletion of ASK1 ameliorates chronic-plus-binge ethanol–induced liver injury. WT and *Ask1*$^{-/-}$ mice were subjected to E10d+1B feeding and were euthanized at 9 hours after gavage. (**A**) Serum ALT levels and circulating neutrophil percentage were measured. (**B**) Liver tissues were subjected to IHC staining with anti-MDA and anti–4-HNE antibodies. Representative images (scale bars: 100 μm) and quantification of areas positive for staining are shown. Values represent mean ± SEM (each dot represents 1 mouse sample). Statistical evaluation was performed by Student's *t* test. *$P < 0.05$, **$P < 0.01$.

treatment with ASK1 inhibitors. Unexpectedly, hepatic expression of BCL2 was elevated in the ASK1 inhibitor groups (Figure 5B). Finally, a reduced number of apoptotic TUNEL$^+$ hepatocytes was observed in ethanol-fed mice after ASK1 inhibitor compared with vehicle treatment (Supplemental Figure 5E).

Genetic deletion of the p38a gene in hepatocytes ameliorates ALD in chronic-plus-binge ethanol–fed mice. To further examine the role of hepatic p38 MAPK, downstream of ASK1, in the pathogenesis of ALD, we generated mice with hepatocyte-specific deletion of p38α (*p38a*$^{Hep-/-}$ mice) (p38α is the major form of p38 MAPKs in the liver) (18). As illustrated in Figure 6A, serum ALT levels as well as circulating neutrophil counts were markedly lower in *p38a*$^{Hep-/-}$ compared with WT mice when they were treated with E10d+1B. The number of MPO$^+$ neutrophils in the liver as well as hepatic expression of *Ly6g* were significantly reduced in *p38a*$^{Hep-/-}$ mice (Figure 6, B and C). Similarly, F4/80$^+$ macrophage infiltration decreased significantly; however, hepatic expression of *F4/80* was similar in *p38a*$^{Hep-/-}$ and WT mice (Figure 6, B and C). Hepatic expression of several proinflammatory mediators is shown in Figure 6C. Expression of *Il6* and *Mip2* was significantly lower in ethanol-fed *p38a*$^{Hep-/-}$ mice than in ethanol-fed WT mice. There was a trend toward a decrease in the expression of *Tnfa*, *Mip1a*, and *Mcp1* in *p38a*$^{Hep-/-}$ mice, although this difference was not statistically significant (Figure 6C). Furthermore, a significant reduction in oxidative stress was observed in *p38a*$^{Hep-/-}$ compared with WT mice after ethanol feeding, as evidenced by the expression of hepatic 4-HNE and MDA based on IHC staining (Figure 6D). In contrast, there was no significant difference in hepatic expression of several phagocytic oxidase units and ER stress–associated genes in *p38a*$^{Hep-/-}$ mice compared with WT mice after E10d+1B treatment, except for the significant downmodulation of *Ero1b* in *p38a*$^{Hep-/-}$ mice (Supplemental Figure 6, A and B).

Treatment with p38α inhibitors ameliorates ALD in chronic-plus-binge ethanol–fed mice. To further dissect the role of p38 in ALD, we employed a pharmacological approach by treating ethanol-fed mice with p38 inhibitors: LY2228820, PH797804, and SB239063. A significant reduction in hepatic activation of p38 was observed after p38 inhibitor treatment (Supplemental Figure 7A). Interestingly, inhibition of p38 also resulted in decreased phosphorylation of ASK1 (Thr838) (Supplemental Figure 7A). In agreement with the observation in *p38a*$^{Hep-/-}$ mice, a significant reduction in serum ALT levels and the percentage of circulating neutrophils was observed in C57BL/6J mice treated with LY2228820 and PH797804 compared with controls (Figure 7A). Yet no significant change in serum ALT levels and circulating neutrophil counts was found in mice treated with SB239063 (Figure 7A). Furthermore, hepatic infiltration of MPO$^+$ neutrophils was lower in all groups treated with p38 inhibitors compared with those with vehicle treatment (Figure 7B), while hepatic expression of *Ly6g* was only significantly reduced in the PH797804-treated group (Figure 7C). Approximately 2- and 1.5-fold reductions in infiltrated F4/80$^+$ macrophages were found in the LY2228820 and SB239063 treatment groups, respectively (Figure 7B); hepatic expression of *F4/80* mRNA was significantly (2-fold) downregulated in the LY2228820 treatment group but not in the PH797804 and SB239063 treatment groups (Figure 7C). We next examined whether the decrease in neutrophil and macrophage infiltration in the liver was secondary to downregulation of inflammatory mediators in the liver.

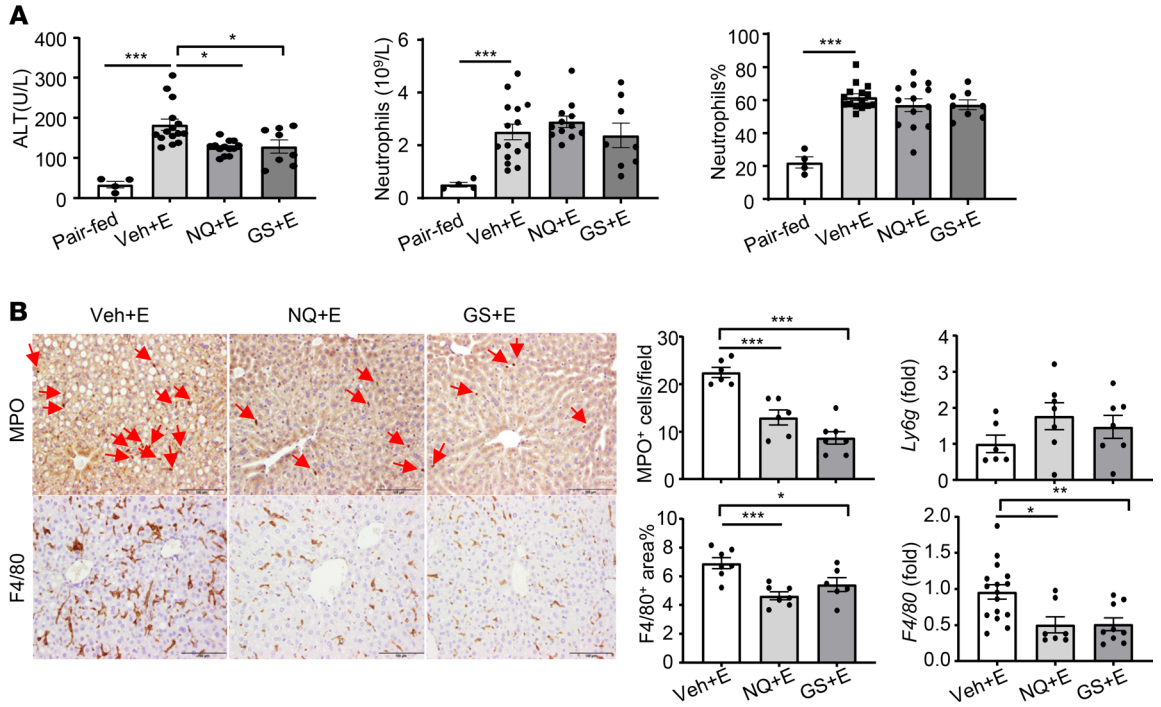

Figure 4. Inhibition of ASK1 ameliorates chronic-plus-binge ethanol–induced hepatic inflammation. C57BL/6J mice were subjected to E10d+1B feeding and received i.p. injection of ASK1 inhibitors (3 mg/kg GS-4997 [GS+E] or 4 mg/kg NQDI-1 ,NQ+E]) 30 minutes before gavage. Mice were euthanized 9 hours after gavage. Veh, vehicle. (**A**) Serum ALT levels and circulating neutrophils were quantified. (**B**) Hepatic neutrophils and macrophages were examined by IHC staining with anti-MPO or anti-F4/80 antibody or by RT-qPCR analysis of *Ly6g* and *F4/80* mRNA. Representative images (scale bars: 100 μm) and quantification of the area positive for each staining are shown. Values represent mean ± SEM (each dot represents 1 mouse sample). Arrowheads indicate MPO⁺ cells. Statistical evaluation was performed by 1-way ANOVA with Tukey's post hoc test for multiple comparisons. $^*P < 0.05$, $^{**}P < 0.01$, $^{***}P < 0.001$.

RT-qPCR analysis demonstrated that LY2228820 treatment downregulated most of the hepatic inflammatory cytokines, except for *Il1b* and *Icam1*. PH797804 treatment only led to the reduction of *Il6* and *Il1b*, and SB239063 treatment had no effect on inflammatory cytokine gene expression (Figure 7C). We also evaluated the effect p38 inhibitors on oxidative stress in the liver of E10d+1B–fed mice. As shown in Figure 8A, levels of hepatic 4-HNE and MDA expression markedly decreased in mice treated with p38 inhibitors. In particular, LY2228820 was the most potent oxidative stress inhibitor, as demonstrated by 12- and 13-fold reductions in the expression of 4-HNE and MDA, respectively (Figure 8A). Additionally, an apparent decrease in hepatic expression of NADPH-associated molecules units — $p47^{phox}$, $p67^{phox}$, $p22^{phox}$, $p40^{phox}$, and $gp91^{phox}$ — was observed only in LY2228820-treated mice (Supplemental Figure 7B). We also found differential effects of each p38 inhibitor on the expression of hepatic *Mt1* and *Mt2*. LY2228820 treatment led to the induction of *Mt1* and *Mt2* by 2- and 1.7-fold, respectively, compared with vehicle treatment, while PH797804 treatment led to a reduction in their expression (Supplemental Figure 7B). Last, treatment with SB239063 had no effect on either *Mt1* or *Mt2* expression (Supplemental Figure 7B). Moreover, LY2228820 treatment led to a significant decrease in hepatic ER stress, as demonstrated by a reduction in protein and mRNA levels of CHOP (Figure 8B and Supplemental Figure 7C). LY2228820 treatment attenuated levels of p-eIF2α protein without affecting total eIF2α protein (Figure 8B).

Deletion or inhibition of ASK1 and p38 decreases mtDNA-enriched EVs in chronic-plus-binge ethanol–fed mice. We have previously demonstrated that chronic-plus-binge ethanol exposure elevates serum levels of mtDNA-enriched EVs in an ER stress–dependent manner, leading to liver inflammation and hepatocyte injury (8). We therefore reasoned that the amelioration of alcohol-induced liver injury by inhibition of ASK1 or p38 may be secondary to the reduction in mtDNA-enriched EV release. Compared with WT mice, $Ask1^{-/-}$ and $p38a^{Hep-/-}$ mice had significantly lower levels of serum EVs and lower mtDNA load in these EVs, as determined by the quantification of cytochrome *c* oxidase (Figure 9A). Similar observations were made in mice treated with either an ASK1 or p38 inhibitor (Figure 9B). Next we asked whether ASK1/p38 pathway-mediated neutrophilia and liver injury are indeed

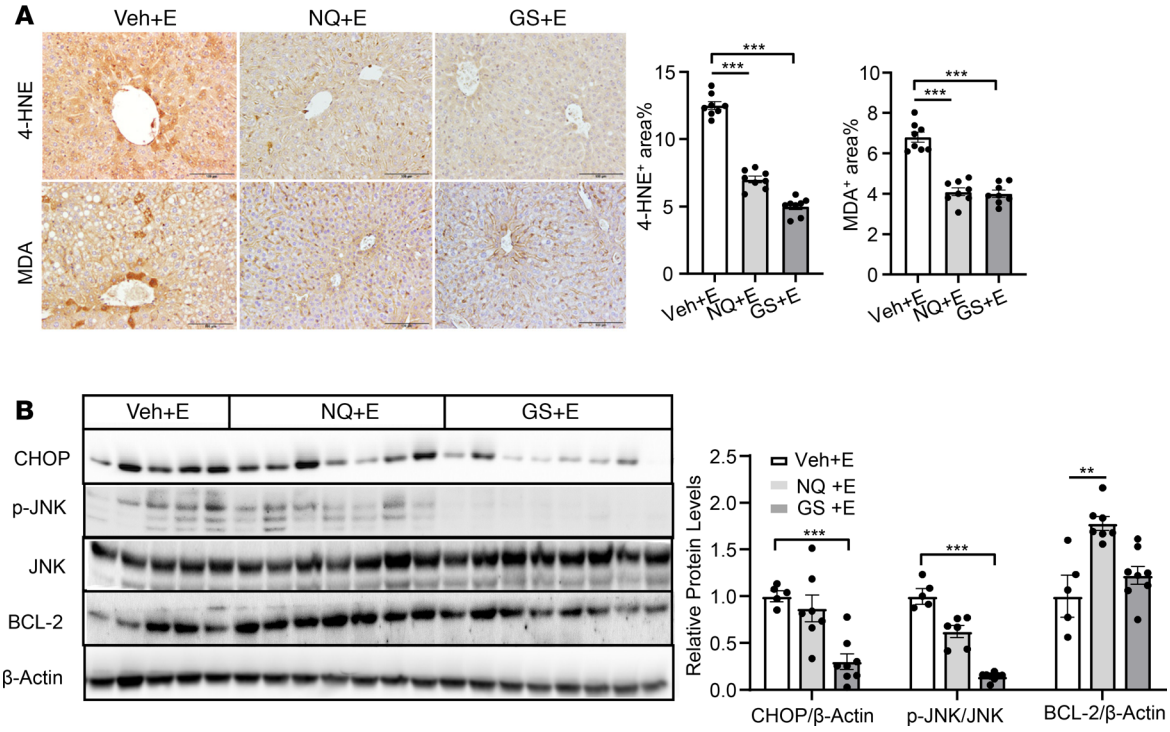

Figure 5. Inhibition of ASK1 ameliorates chronic-plus-binge ethanol–induced hepatic oxidative stress and ER stress. C57BL/6J mice were subjected to E10d+1B feeding and received i.p. injection of ASK1 inhibitors (3 mg/kg GS-4997 or 4 mg/kg NQDI-1) 30 minutes before gavage. Mice were euthanized 9 hours after gavage. (**A**) Liver tissues were subjected to immunostaining with antibody against MDA or 4-HNE. Representative images (scale bars: 100 μm) and quantification of the area positive for each staining are shown. (**B**) Western blot analysis of CHOP, BCL2, p-JNK, JNK, and β-actin in the liver. Values represent mean ± SEM (each dot represents one mouse sample). Statistical evaluation was performed by 1-way ANOVA with Tukey's post hoc test for multiple comparisons. $^{**}P < 0.01$, $^{***}P < 0.001$.

mediated by mtDNA-enriched EVs. To test this hypothesis, we purified mtDNA-enriched EVs from the serum of E10d+1B-treated WT and *Ask1*$^{-/-}$ mice and injected these EVs into chronically ethanol-fed C57BL/6J mice (E10d). As illustrated in Supplemental Figure 8, injection of E10d+1B-treated WT mouse EVs induced a greater number and percentage of circulating neutrophils than injection of E10d+1B-treated *Ask1*$^{-/-}$ mouse EVs. However, the 2 types of EVs caused similar elevations in serum ALT levels in ethanol-fed mice. The lack of difference in serum ALT levels between these 2 groups may be because multiple pathways contribute to chronic-plus-binge ethanol–induced liver injury in addition to neutrophils.

To confirm that deficiency in *Ask1* and *p38a* led to the reduction in the release of EVs and EV-containing mtDNA from hepatocytes, we isolated primary hepatocytes from WT, *Ask1*$^{-/-}$, or *p38a*$^{Hep-/-}$ mice and treated them with either PBS or ethanol (100 mM for 24 hours). The quantity of EVs and EV-containing mtDNA was then determined from the supernatants. We found a significant reduction in the quantity of EVs released from the primary *Ask1*$^{-/-}$ or *p38a*$^{Hep-/-}$ hepatocytes treated either with PBS or ethanol compared with WT hepatocytes (Figure 9C). Moreover, treatment with ASK1 inhibitors (GS-4997 or NQDI-1) or p38 inhibitors (LY2228820 or PH797804) markedly reduced the number of EVs and EVs-containing mtDNA in the supernatant of primary WT hepatocytes (Figure 9, D and E).

Inhibition of ASK1 or p38 downregulates expression of EV biogenesis– and secretion–related genes in chronic-plus-binge ethanol–fed mice. To understand how the ASK1/p38 pathway affects EV release and biogenesis in ethanol-fed mice, we performed RT-qPCR analyses of multiple genes related to EV biogenesis and trafficking processes (30). EV formation involves endosomal sorting complex required for transport (ESCRT) machinery, either in a dependent or independent manner. In the ESCRT-dependent pathway, 4 different protein complexes, ESCRT-0, -I, -II, and -III, and the associated AAA ATPase Vps4 complex act with other accessory proteins to drive multivesicular body (MVB) formation by invagination and scission of endosomal membranes (31). Certain ESCRT components, such as TSG101 (ESCRT-1) and ALIX (an ESCRT accessory protein), are commonly found in exosomes themselves. EVs can be

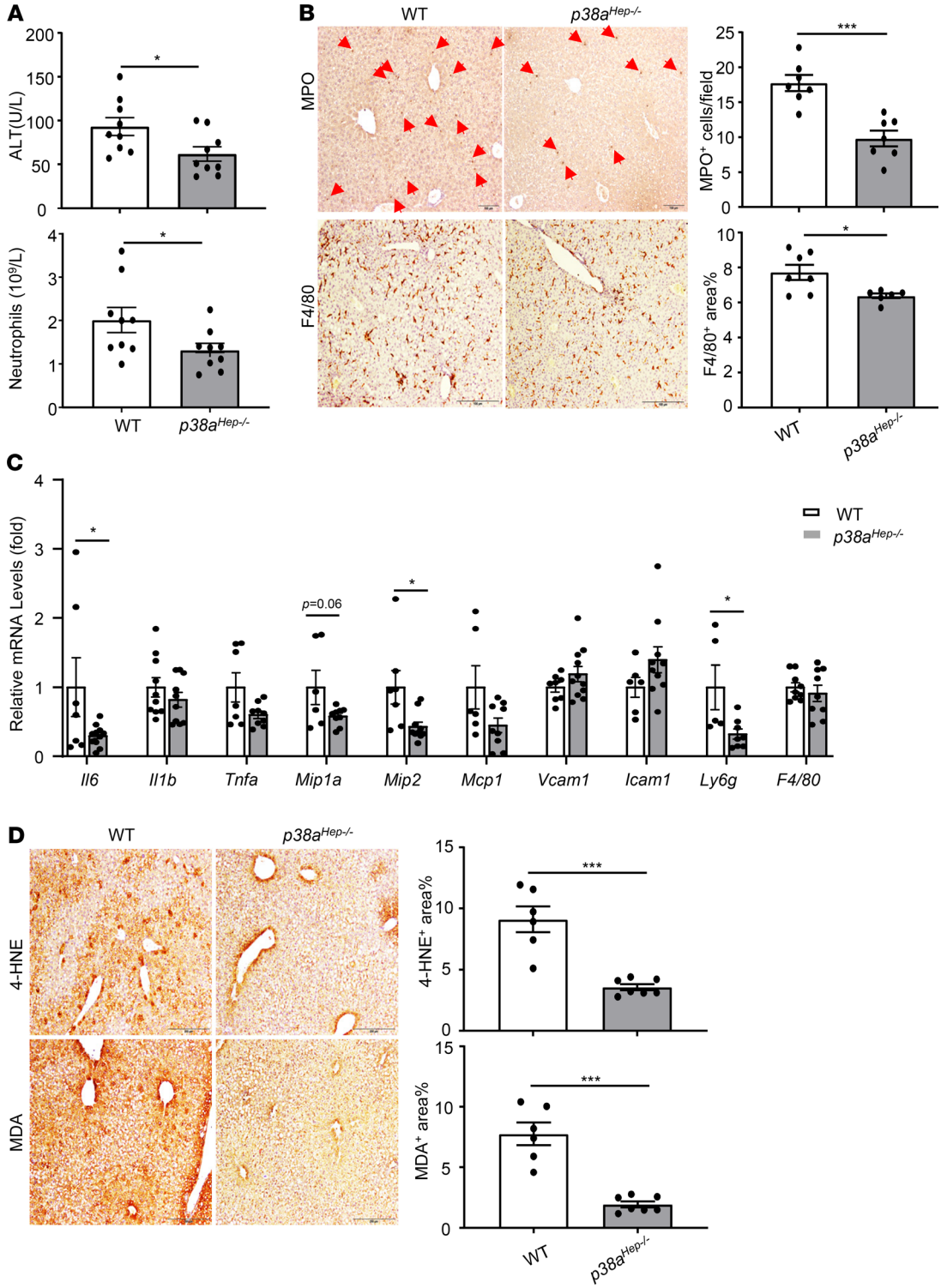

Figure 6. Hepatocyte-specific deletion of the *p38a* gene ameliorates chronic-plus-binge ethanol–induced liver injury. WT and *p38a*$^{Hep-/-}$ mice were subjected to E10d+1B feeding and were euthanized 9 hours after gavage. (**A**) Serum ALT levels and circulating neutrophils were quantified. (**B**) Liver tissues were subjected to IHC staining with antibodies against MPO and F4/80. Representative images (scale bars: 200 μm) and quantification of MPO$^+$ cells and F4/80$^+$ area (%) are shown. (**C**) Liver tissues were subjected to RT-qPCR analysis of inflammatory cytokine genes. (**D**) Liver tissues were subjected to immunostaining with antibodies against MDA and 4-HNE. Representative images (scale bars: 200 μm) and quantification of the area positive for each staining are shown. Values represent mean ± SEM (each dot represents 1 mouse sample). Statistical evaluation was performed by Student's *t* test. $^*P < 0.05$, $^{***}P < 0.001$.

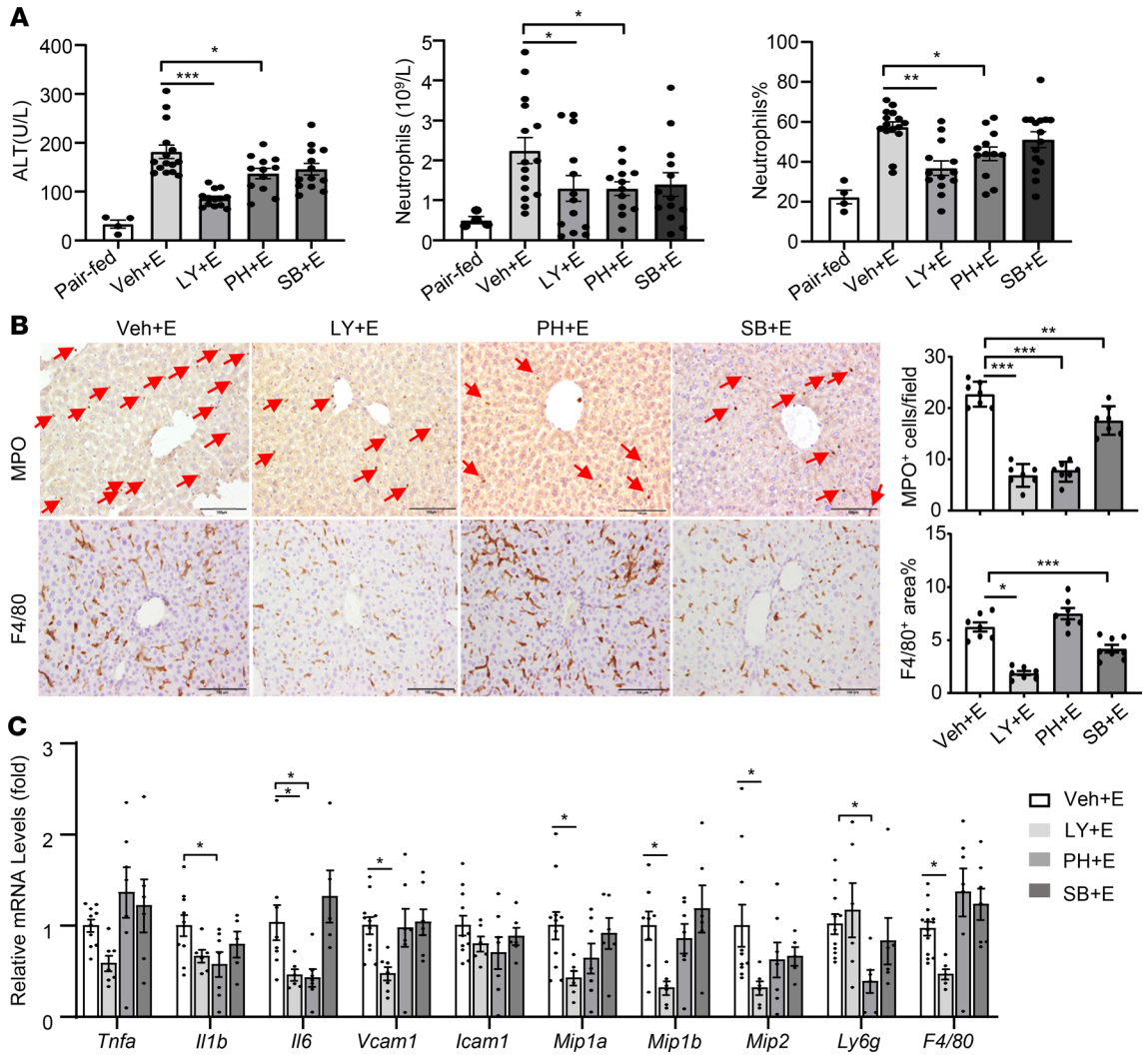

Figure 7. Treatment with p38 inhibitors ameliorates chronic-plus-binge ethanol–induced hepatic inflammation. C57BL/6J mice were subjected to E10d+1B feeding and received i.p. injection of p38 inhibitors (3 mg/kg LY2228820 [LY+E], 12 mg/kg PH797804 [PH+E], or 10 mg/kg SB239063 [SB+E]) 30 minutes before gavage. Mice were euthanized 9 hours after gavage. (**A**) Serum ALT levels and circulating neutrophils were measured. (**B**) Liver tissues were subjected to IHC staining with antibody against MPO or F4/80. Representative images are shown (scale bars: 100 μm). (**C**) RT-qPCR was performed to analyze hepatic expression of proinflammatory mediators. Values represent mean ± SEM (each dot represents 1 mouse sample). Statistical evaluation was performed by 1-way ANOVA with Tukey's post hoc test for multiple comparisons. $^*P < 0.05$, $^{**}P < 0.01$, $^{***}P < 0.001$.

also formed in an ESCRT-independent manner. In this pathway, ceramide is generated from sphingomyelin via the action of neutral sphingomyelinase 2 (NSMase2), and inhibition of this enzyme or gene knockdown has been shown to block exosome release or exosome-mediated signaling in some cell types (32, 33). Additionally, many small Rab GTPases play important roles in exosome production because they regulate intracellular trafficking of endosomes (from which MVBs originate) as well as transport of vesicles to the plasma membrane and their subsequent release from the cell (34). Rab27a and Rab27b are essential for exosome secretion (35).

To explore underlying mechanisms related to EV biogenesis, we performed RT-qPCR analyses of vesicle-trafficking Rab GTPases (*Rab27a*, *Rab27b*, *Rab5b*, *Rab11a*, *Rab11b*, *Rab35*), and components of the ceramide (*Smpd3*), ESCRT (*Hgs*, *Alix*, *Stam1*, *Tsg101*, *Pdcd61p*, *Vta1*, *Ykt6*), and VAMP family (*Vamp7, Vamp8*) genes. Our data revealed that hepatic expression of Rab GTPases (*Rab27a*, *Rab27b*, *Rab5b*, *Rab11a*, *Rab35*) and genes related to ESCRT (*Hgs*, *Pdcd61p*, *Stam1*, *Ykt6*) was lower in ethanol-fed *Ask1*$^{-/-}$ mice than in ethanol-fed WT mice (Figure 10A). Findings were similar in ethanol-fed *p38a*$^{Hep-/-}$ compared with WT mice (Figure 10B). Additionally, we found lower expression levels of some EV biogenesis–related genes in ethanol-fed mice treated with ASK1 or p38 inhibitor compared with those treated with vehicle (Figure 10, C and D).

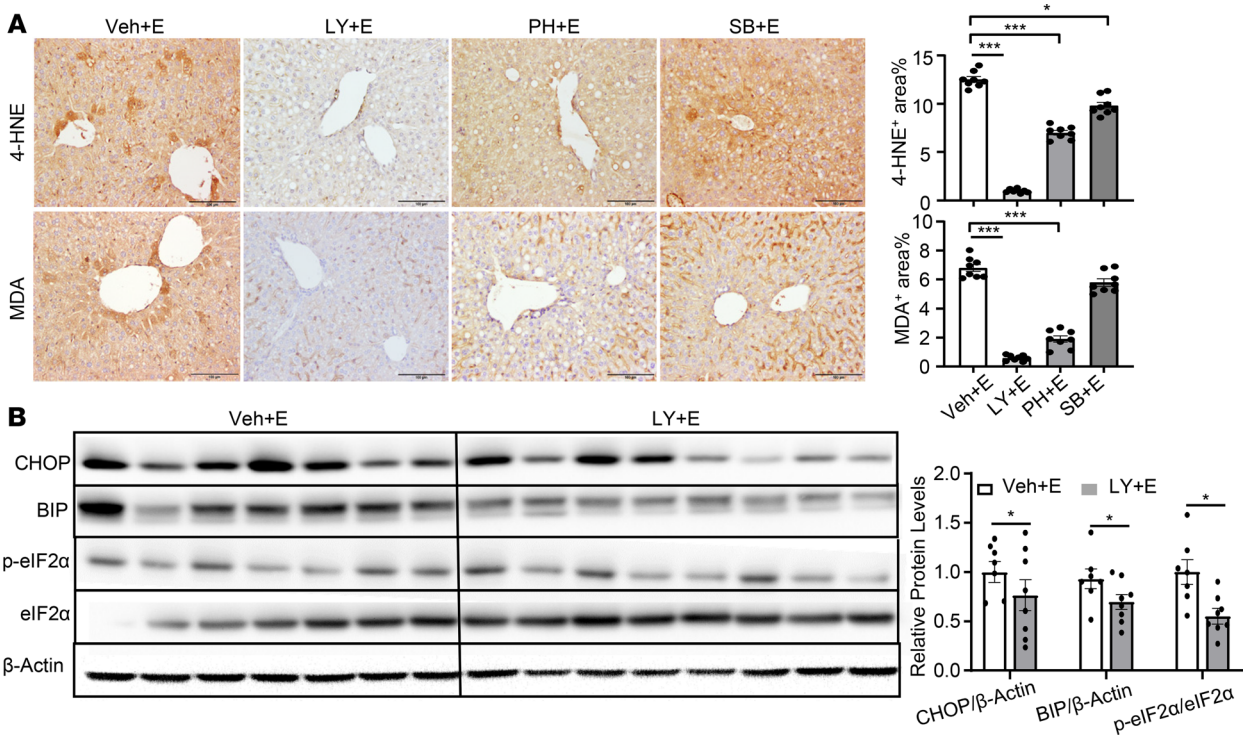

Figure 8. Treatment with p38 inhibitors ameliorates chronic-plus-binge ethanol–induced hepatic oxidative stress and ER-stress. C57BL/6J mice were subjected to E10d+1B feeding and received i.p. injection of p38 inhibitors (3 mg/kg LY2228820, 12 mg/kg PH797804, or 10 mg/kg SB239063) 30 minutes before gavage. Mice were euthanized 9 hours after gavage. (**A**) Liver tissues were subjected to immunostaining with antibody against MDA and 4-HNE. Representative images (scale bars: 100 μm) and quantification of the area positive for each staining are shown. (**B**) Western blot analysis of CHOP, BIP, p-eIF2α, total eIF2α, and β-actin in the liver. Values represent mean ± SEM (each dot represents 1 mouse sample). Statistical evaluation was performed by 1-way ANOVA with Tukey's post hoc test for multiple comparisons. $^{*}P < 0.05$, $^{***}P < 0.001$.

Furthermore, we performed Western blot analyses to confirm the changes in protein expression related to the biogenesis or transportation of EVs. As illustrated in Supplemental Figure 9, treatment with ASK1 or p38 inhibitor markedly reduced expression of NSMase2, ALIX, and Rab27A proteins in AML12 cells (Supplemental Figure 9).

Discussion

Neutrophil infiltration is the pathological hallmark of alcoholic steatohepatitis; however, the mechanisms underlying hepatic neutrophil infiltration have not been fully elucidated. In this study, we examined oxidative stress–associated genes after chronic-plus-binge ethanol feeding by microarray analysis and found *Mt1* and *Mt2* genes were the 2 most highly elevated oxidative-stress–related genes. MT1 and MT2 are small, cysteine-rich proteins that play an important role in the intracellular stress response (36). Zhou et al. previously reported that ethanol intake–induced liver injury was exacerbated in *Mt1/2*-KO mice but reduced in *Mt*-transgenic mice (37, 38). Here we found that deletion of the *Mt1* and *Mt2* genes aggravated alcohol-induced liver inflammation, injury, and oxidative stress after ethanol feeding, and subsequently enhanced activation of the stress kinases ASK1 and p38 in the liver. We further provide evidence suggesting that activation of the ASK1/p38 pathway induced mtDNA damage and release via EVs, and that these mtDNA-enriched EVs contribute to neutrophil infiltration in the liver.

The ASK1 pathway is thought to coordinately regulate gene expression, mitosis, metabolism, motility, survival, apoptosis, and differentiation (39). ASK1 has been considered to be the potential therapeutic target for patients with severe alcoholic hepatitis, and an ASK1 inhibitor, selonsertib (GS-4997), was administered to patients with severe alcoholic hepatitis in a recent phase II clinical study (40). Unfortunately, this study did not demonstrate favorable outcomes, as patients developed bacterial infection, and no improvement in mortality or liver function was observed (40). However, the pivotal role of ASK1 cannot be neglected; indeed, researchers remain committed to ASK1-targeted therapies in human disease. Schuster-Gaul et al.

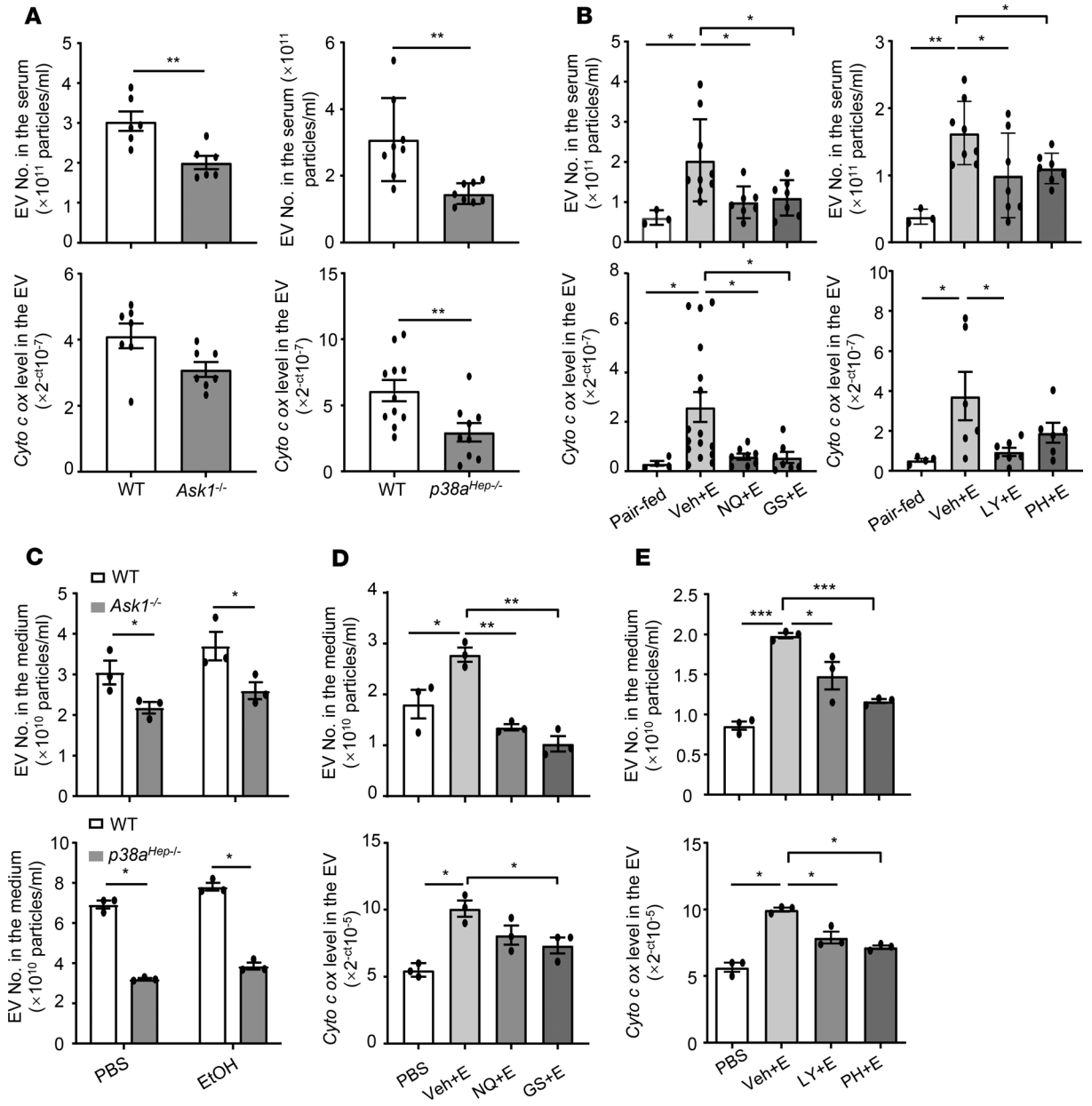

Figure 9. ASK1/p38 pathway activation contributes to elevated release of mtDNA enriched EVs in E10d+1B model. (**A**) WT, *Ask1*$^{-/-}$, and *p38a*$^{Hep-/-}$ mice were subjected to E10+1B ethanol feeding and were euthanized 9 hours after gavage. Serum EVs were isolated and quantified by exosome quantitation assay. Cytochrome *c* oxidase (*Cyto c ox*) DNA levels in EVs were measured. (**B**) C57BL/6J mice were subjected to E10d+1B feeding and received i.p. injection of ASK1 or p38 inhibitors 30 minutes before gavage. Mice were euthanized 9 hours after gavage. Serum EVs were isolated and counted by exosome quantitation assay. *Cyto c ox* DNA levels in EVs were measured. (**C**) Hepatocytes were isolated from WT, *Ask1*$^{-/-}$, or *p38a*$^{Hep-/-}$ mice and treated with ethanol (100 mM) or PBS for 24 hours. EVs were isolated from culture medium and counted by exosome quantitation assay. (**D** and **E**) Hepatocytes were isolated from WT mice and treated with ethanol (100 mM) or ethanol plus ASK1 or p38 inhibitors for 24 hours. EVs were isolated from culture medium and counted by exosome quantitation assay. *Cyto c ox* DNA levels in the EVs were measured. Values represent mean ± SEM (each dot represents 1 mouse sample). Statistical evaluation was performed by Student's *t* test or 1-way ANOVA with Tukey's post hoc test for multiple comparisons. $^*P < 0.05$, $^{**}P < 0.01$, $^{***}P < 0.001$.

found that pharmacologic inhibition of ASK1 could attenuate liver cell death and hepatic fibrosis driven by inflammasome activation using gain-of-function NOD-like receptor protein 3 (*Nlrp3*) mutant mice, providing mechanistic insight into the antifibrotic mechanisms of ASK1 inhibition (41). In the current study, we demonstrated that ASK1 plays an important role in promoting oxidative stress and liver injury in chronic-plus-binge ethanol–fed mice. Inhibition or genetic deletion of ASK1 ameliorated liver injury in the E10+1B model as evidenced by decreased serum ALT, oxidative stress, and ER stress and reduced hepatic neutrophil

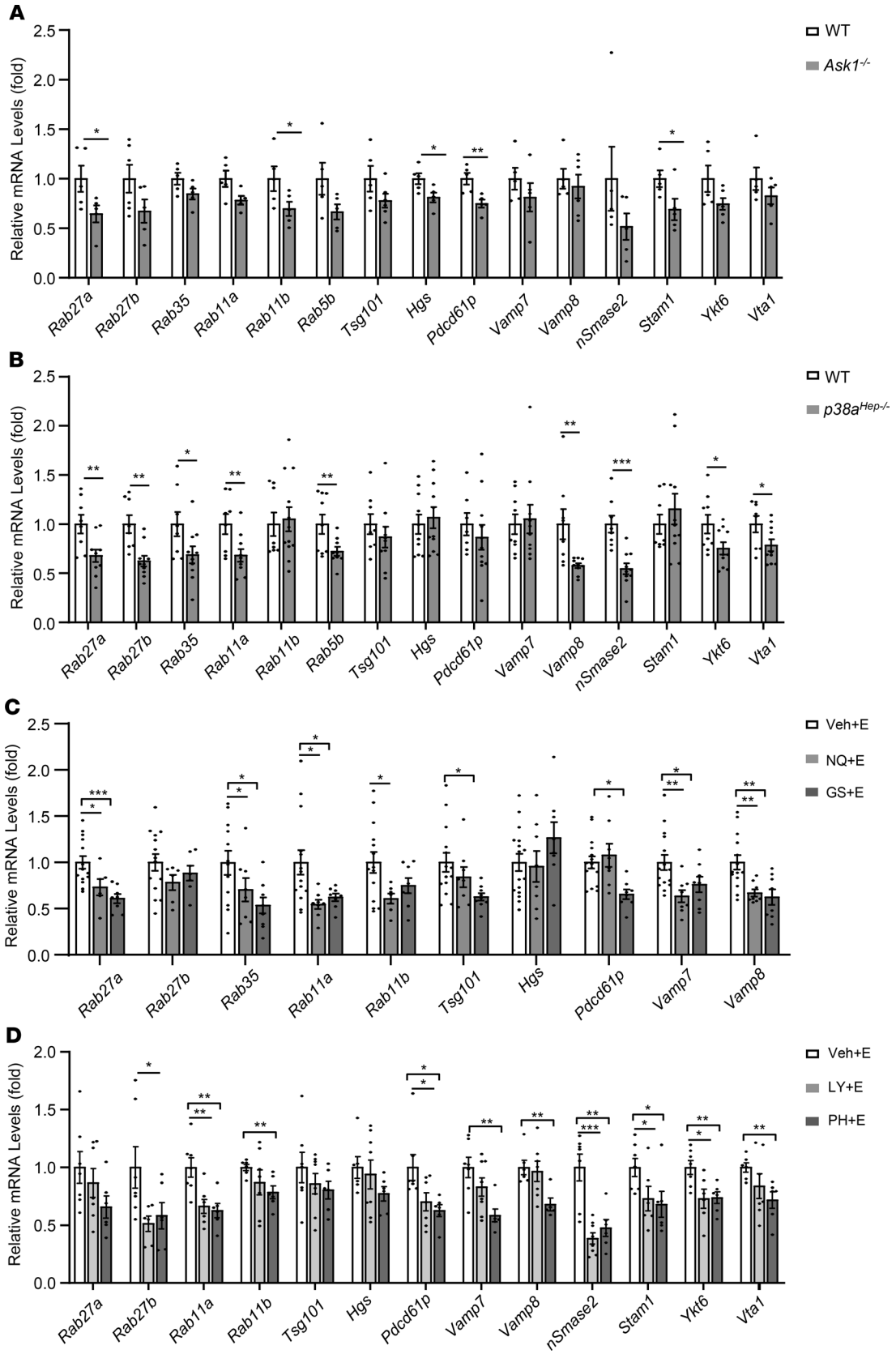

Figure 10. Inhibition of ASK1 or p38 activation attenuates expression of the genes related to EV biogenesis and secretion in the E10d+1B model. (**A** and **B**) WT and *Ask1*$^{-/-}$ or *p38a*$^{Hep-/-}$ mice were subjected to E10d+1B feeding and euthanized 9 hours after gavage. Liver tissues were subjected to RT-qPCR analysis of EV biogenesis– and secretion–related genes. (**C** and **D**) C57BL/6J mice were subjected to E10d+1B feeding and received i.p. injection of ASK1 inhibitor (3 mg/kg GS-4997 or 4 mg/kg NQDI-1) or p38 inhibitor (3 mg/kg LY2228820 or 12 mg/kg PH797804) 30 minutes before gavage. Mice were euthanized 9 hours after ethanol gavage Liver tissues were subjected to RT-qPCR analysis of EV biogenesis– and secretion– related genes. Values represent mean ± SEM (each dot represents 1 mouse sample). Statistical evaluation was performed by Student's *t* test or 1-way ANOVA with Tukey's post hoc test for multiple comparisons. $^{*}P < 0.05$, $^{**}P < 0.01$, $^{***}P < 0.001$.

and macrophage infiltration. Our data suggest the possible beneficial roles of ASK1 inhibitors in the early stages of alcoholic steatohepatitis (as indicated by our chronic-plus-binge ethanol–fed model) but not in the severe form of the disease with advanced fibrosis/cirrhosis, inflammation, and bacterial infection (as those who were enrolled in the aforementioned phase II clinical trial) (40).

ROS can activate not only ASK1 but also other downstream kinases that may accelerate the progression of alcoholic steatohepatitis. The p38 MAPKs are known to be activated by MEK3 (or MKK3) and MEK6 (or MKK6); both MEK2 and MEK6 can be activated by one of the several upstream MAP3Ks, such as ASK1, dual-leucine zipper-bearing kinase 1 (DLK1), and TFG-β–activated kinase 1 (TAK1) (18). Once activated by MKK3 or MKK6, p38 MAPKs can potentiate the downstream signals or activate other proteins directly (42). The p38 family comprises 4 members, p38α (19), p38β (43–45), p38γ (46), and p38δ (47, 48), which have been implicated in various cellular responses controlling cell proliferation, differentiation, apoptosis, embryogenesis, inflammatory responses, and stress responses in human reproductive tissues. A large body of evidence indicates that p38 activity is critical for normal immune and inflammatory responses (42). In our study, we focused on specific roles of hepatic p38α and its implication in the progression of alcoholic steatohepatitis. Our data revealed that hepatocyte-specific deletion of *p38a* or administration of p38 inhibitors markedly ameliorated serum ALT levels, oxidative stress, as well as ER stress, suggesting the role of hepatic p38–induced liver injury and inflammation in the chronic-plus-binge ethanol–feeding model. Interestingly, although ethanol-fed $p38a^{Hep-/-}$ mice had lower serum ALT levels than ethanol-fed WT mice, hepatic steatosis was greater in $p38a^{Hep-/-}$ mice than in WT mice (our unpublished data). These findings suggest that hepatic p38α plays distinct roles in controlling steatosis and liver injury in ALD, which is consistent with our recent studies indicating that hepatocyte-specific deletion of *p38a* increases simple steatosis but ameliorates oxidative stress–driven nonalcoholic steatohepatitis (NASH) in the HFD^{+Cxcl1}-induced nonalcoholic fatty liver disease (NAFLD) model (49). In addition, treatment with p38 inhibitors induced greater amelioration of ethanol-induced liver injury than genetic deletion of the *p38a* gene in hepatocytes. This is likely due to the effect of p38 inhibitors on other cell types in addition to hepatocytes that may contribute to alcohol-induced liver injury and inflammatory processes. Indeed, a recent study reported that macrophage p38α promoted the progression of steatohepatitis by inducing proinflammatory cytokine secretion and M1 polarization (26).

Although p38 has been implicated in various cellular responses including cell death and oxidative stress (42), the exact mechanisms by which p38 activation affects hepatocytes remain obscure. Wang et al. (50) reported that p38 was involved in cyclophilin D stimulation of permeability transition pore excessive opening, subsequently causing ER stress and hepatic steatosis. In the current study, we demonstrated that p38 activation promoted mtDNA damage in hepatocytes, which was then released via EVs and subsequently induced neutrophil activation. EVs are emerging as new players in the investigation of intercellular communication. Our mechanistic studies found that inhibition and genetic deletion of *Ask1* and *p38a* ameliorated ethanol-induced liver injury by downregulating mtDNA-enriched EVs — one of the key factors in promoting ethanol-induced hepatic neutrophil infiltration and liver injury in the chronic-plus-binge ethanol feeding model (8). It is conceivable that attenuated ER stress and mitochondrial damage contributed to the decreased production of mtDNA-enriched EVs that occurred after ablation of ASK1 and p38 function. In addition, we also found that ethanol-mediated induction of EVs in circulation either in vivo or in hepatocytes in vitro was decreased after inhibition of ASK1 or p38, suggesting that the ASK1/p38 pathway plays an important role in the biogenesis of hepatocyte-derived EVs. Previous studies reported that inhibition of p38 in human aortic endothelial cells resulted in a 50% reduction in TNF-α–induced EVs (51). Additionally, p38 is essential for P2X7-dependent NSMase translocation to the plasma membrane, and its inhibition blocks capsaicin-induced EV shedding from microglia in vitro and in cortical brain slices (52, 53). The ability of EVs to transfer cargo from donor to acceptor cells, thereby triggering phenotypic changes in the latter, has generated substantial interest in the scientific community. We and others have previously demonstrated that mtDNA-enriched EVs released by hepatocytes are able to induce neutrophil activation, resulting in liver inflammation (8, 54). In addition, mtDNA can also induce NLRP3 inflammasome activation through engagement of Toll-like receptors in macrophages (55) and promote neutrophil extracellular trap formation, contributing to the progression of diseases (56–58). It will be interesting to examine whether these mechanisms also contribute to liver inflammation and injury induced by mtDNA-enriched EVs after chronic-plus-binge ethanol feeding.

In conclusion, our findings indicate that activation of ASK1 and p38 mediates alcoholic liver injury and inflammation by promoting proinflammatory mtDNA-enriched EV release in hepatocytes induced by ROS stress and ER stress. Despite the failure of anti-ASK1 therapy for patients with severe alcoholic hepatitis in a recent clinical trial (40), our study suggested that ASK1 and p38 activation plays an important role in the pathogenesis of the early stages of alcoholic steatohepatitis. Therapeutic intervention targeting this pathway in patients with a less severe form of alcoholic hepatitis deserves further investigation.

Methods

Mice. C57BL/6J, *Mt1/2*$^{-/-}$, and Albumin-Cre mice were obtained from the Jackson Laboratory. C57BL/6N mice were obtained from Charles River. *Ask1*$^{-/-}$ mice were originally obtained from Hidenori Ichijo (University of Tokyo, Tokyo, Japan) (59). Heterozygous mice were bred to generate *Ask1*$^{-/-}$ mice and their corresponding WT littermate controls. *Mt1/2*$^{-/-}$ mice with deletion of both *Mt1* and *Mt2* genes were backcrossed to a C57BL/6N background for more than 15 generations, and C57BL/6N mice were used as controls. *p38a*-floxed mice were provided by Yibin Wang (UCLA, Los Angeles, California, USA) and were crossed with Albumin-Cre mice via several steps to generate hepatocyte-specific *p38a* deletion. All animals were cared for in accordance with NIH guidelines. Mice were housed in a temperature-controlled room with a 12-hour dark/12-hour light cycle.

Chronic-plus-binge ethanol feeding protocols. The chronic-plus-binge ethanol feeding model was described previously (4, 27). Briefly, 10- to 12-week-old female mice were initially fed a Lieber-DeCarli liquid diet (F1259SP, Bio-Serv) ad libitum for 5 days during acclimatization. Subsequently, the ethanol-fed groups were allowed free access to an ethanol diet (F1258SP, Bio-Serv) containing 5% (v/v) ethanol for 10 days or 8 weeks, then received a single dose of ethanol (5 g/kg body weight) via oral gavage in the early morning and were sacrificed 3, 6, or 9 hours later. In addition, mice were fed an ethanol-containing Lieber-DeCarli diet for 10 days as described for chronic feeding (designated as E10d) or received a single dose of ethanol (5 g/kg body weight) via gavage in the early morning (designated as 1B) and were sacrificed 9 hours later. In some experiments, mice received ASK1 inhibitor GS-4997 at 3 mg/kg or NQDI-1 at 4 mg/kg by i.p. injection; or p38 inhibitor LY2228820 at 3 mg/kg, PH797804 at 12 mg/kg, or SB239063 at 10 mg/kg by i.p. injection approximately 30 minutes before oral gavage. All inhibitors were obtained from Selleck Chemicals.

Microarray analyses of mouse liver samples. Dye-coupled cDNAs were purified with a MiniElute PCR purification kit (QIAGEN) and hybridized to a 44K mouse 60-mer oligo microarray (Agilent Technologies). Data were processed and analyzed using GeneSpring GX software (Agilent Technologies). Full microarray data were deposited in the NCBI's Gene Expression Omnibus database (GEO GSE67546).

Biochemical assays. Serum ALT levels were determined from serum collected from mouse retro-orbital plexus using a Catalyst Dx Chemistry Analyzer (IDEXX Laboratories) according to the manufacturer's instructions.

TBARS assay. Approximately 25-mg liver tissue samples were homogenized or lysed in RIPA buffer containing a cocktail of protease inhibitors (Santa Cruz Biotechnology). The samples were then vortexed and centrifuged at 1600 *g* at 4°C for 10 minutes. The supernatant was used for analysis according to the TBARS assay kit manufacturer's instructions (Cayman).

Liver histology and IHC staining. Liver specimens were fixed in 10% buffered formalin and embedded in paraffin. Then, 4-μm sections were cut and used for IHC staining. TUNEL staining was performed with an ApopTag Peroxidase *In Situ* Apoptosis Detection Kit (Millipore). For IHC, after heat-induced epitope retrieval, paraffin-embedded sections were incubated in 3% H_2O_2 and blocked in 3% normal serum buffer. Sections were incubated with primary antibodies overnight at 4°C. Vectastain Elite ABC Staining Kit and DAB Peroxidase Substrate Kit (Vector Laboratories) were used to visualize the staining according to the manufacturer's instructions, as described previously (60). The following primary antibodies were used: MPO (PP023AA, Biocare Medical), F4/80 (30325, Cell Signaling Technology), MDA (1F83, Genox), 4-HNE (HNEJ-2, Genox), p-ASK1 (PA5-64541, Thermo Fisher Scientific), and p-p38 (4511s, Cell Signaling Technology). Positive cells and positive areas in 10 randomly selected high-power fields were analyzed.

Total RNA isolation and RT-qPCR. Total RNA was purified from liver tissues or cell cultures using TRIzol Reagent (Thermo Fisher Scientific) according to the manufacturer's instructions. RNA (1 μg of total) was reverse transcribed into cDNA using a High-Capacity cDNA Reverse Transcription Kit (Thermo Fisher Scientific). Expression levels of mRNA were measured by RT-qPCR with an ABI7500 RT-PCR system (Applied Biosystems). 18S rRNA was used as the invariant housekeeping control gene. The $2^{-\Delta\Delta Ct}$ method was used to calculate relative gene expression. The primers used for RT-qPCR are listed in Supplemental Table 1.

Western blotting. Liver tissues and cells were homogenized or lysed in RIPA buffer containing a cocktail of protease inhibitors (Santa Cruz Biotechnology) according to the manufacturer's instructions, then vortexed and centrifuged at 10,000 *g* at 4°C for 10 minutes. The protein extracts were mixed in Laemmli loading buffer, boiled for 10 minutes, and then subjected to SDS-PAGE. After electrophoresis on 4%–12% Bis-Tris gel (Bio-Rad), proteins were transferred onto nitrocellulose membranes (Thermo Fisher Scientific) and blotted against the respective primary antibodies overnight. Antibodies against p-p38 (Thr180/Tyr182 (4511s), p38, p-JNK (Thr183/Tyr185) (catalog 4668), JNK (catalog 9252), p-STAT3 (Tyr705) (9145s), STAT3 (catalog 30835), p-PERK (Thr982) (3179s), p-eIF2α (Ser51) (catalog 3398), eIF2α (catalog 5324), CHOP (5554s), BIP (3177s), BCL-2 (3498s), ALIX (catalog 92880), and Rab27A (69295s) were purchased from Cell Signaling Technology. Antibodies against p-ASK1 (Thr838) and ASK1 were purchased from Thermo Fisher Scientific. The antibody against 4-HNE was purchased from Genox. The antibody against NSMase2 was purchased from Santa Cruz Biotechnology. Membranes were washed with 0.1% (v/v) Tween-20 in PBS (pH 7.4) and incubated with a 1:5000 dilution of HRP-conjugated secondary antibody for 1 hour. Protein bands were visualized by SuperSignal West Femto Maximum Sensitivity Substrate (Thermo Fisher Scientific).

Isolation and culture of mouse primary hepatocytes and AML12 cells. For hepatocyte isolation, mice were anesthetized with 30 mg/kg pentobarbital sodium i.p. The portal vein was cannulated and the liver perfused with ethylene glycol tetraacetic acid and subsequently with 0.075% collagenase (Worthington) as previously described (61). Primary hepatocytes were collected after centrifugation at 50 *g* for 5 minutes and cultured in DMEM containing 10% EV-free FBS and penicillin-streptomycin. In some experiments, primary hepatocytes were cultured with either ethanol at 100 mM or ethanol plus 30 μM NQDI-1, 30 μM GS-4997, 2 μM LY2228820, or 4 μM PH797804, respectively, for 24 hours. All inhibitors were obtained from Selleck Chemicals. AML12 cells (mouse hepatocyte cell line) were cultured in a 1:1 mixture of DMEM and Ham's F12 medium with 5 μg/mL insulin, 5 μg/mL transferrin, 5 ng/mL selenium, 40 ng/mL dexamethasone, 10% FBS, and penicillin-streptomycin.

EV isolation and cell treatment. EVs were isolated as previously described (62). Briefly, after centrifugation of serum or cultured medium at 3000 *g* for 15 minutes at 4°C, the supernatant fraction including EVs was incubated with an appropriate volume of ExoQuick or ExoQuick-TC exosome precipitation solution (System Biosciences), depending on the type of samples for EV isolation procedure, according to the manufacturer's manual. The size of EVs was assessed using a NanoSight NS300 System (Malvern Instruments) equipped with a fast video capture and nanoparticle tracking analysis, and the concentration of EVs was measured using a Pierce BCA protein assay Kit (Thermo Fisher Scientific) and EXOCET Exosome Quantitation Kit (System Biosciences).

Injection of serum EVs. EVs were isolated from 1 mL serum from E10d+1B-fed WT and *Ask1*$^{-/-}$ mice as described above and then measured using an EXOCET Exosome Quantitation Kit (System Biosciences). The EV pellets (~1×10^{12} particles) were resuspended in 150 μL PBS and injected through the tail vein into E10d-fed C57BL/6J mice.

Quantification of mtDNA in EVs. After quantification of EVs using a BCA protein assay, an equal amount of EVs was subjected to DNA extraction using a QIAmp DNA Mini Kit (QIAGEN) as previously described (62). The extracted DNA was further quantified using NanoDrop spectrometer (Thermo Fisher Scientific), and an equal amount of DNA was subjected to real-time PCR reaction using the primers for mitochondrial genome–specific genes (e.g., cytochrome *c* oxidase). The primer sequences used for PCR reactions are listed in Supplemental Table 1.

Statistics. Results are expressed as mean ± SEM. All statistical analyses were performed using GraphPad Prism software (v. 7.0a; GraphPad Software). To compare values obtained from 2 groups, 2-tailed Student's *t* test was performed. Data from multiple groups were compared with 1-way ANOVA followed by post hoc analysis with Tukey's test, as appropriate. *P* values less than 0.05 were considered significant.

Study approval. Animal care and experiments were conducted under guidelines and protocols approved the National Institute on Alcohol Abuse and Alcoholism (NIAAA) Animal Care and Use Committee.

Author contributions

JM and HC designed and conducted the experiments and wrote the manuscript; RMR and SL helped with the experiment design, performed data analysis and edited the manuscript; MX, TR, YH, SH, DF, RR, and PY conducted some experiments; JS and BG are co-advisors for JM's PhD thesis, supervised the entire study, and edited the manuscript.

Acknowledgments

The authors are grateful to Yibin Wang (University of California, Los Angeles) for providing *p38a*-floxed mice and to the laboratory members for critical reading of the manuscript. This work was supported in part by the intramural program of the NIAAA, NIH (to BG), and National Science and Technology Major Project (2017ZX10202202 to JS) in the Southern Medical University (SMU), Guangzhou, China. JM was affiliated with the SMU and the NIH Graduate Partnerships Program. JM was a participant in the NIH Graduate Partnerships Program and a graduate student in the SMU.

Address correspondence to: Bin Gao, Laboratory of Liver Diseases, NIAAA/NIH, 5625 Fishers Lane, Bethesda, Maryland 20892, USA. Email: bgao@mail.nih.gov. Or to: Jian Sun, Department of Infectious Diseases, Nanfang Hospital, Southern Medical University, Guangzhou, China. Email sunjian@fimmu.edu.cn.

1. Gao B, Bataller R. Alcoholic liver disease: pathogenesis and new therapeutic targets. *Gastroenterology*. 2011;141(5):1572–1585.
2. Szabo G, Kamath PS, Shah VH, Thursz M, Mathurin P, EASL-AASLD Joint Meeting. Alcohol-related liver disease: areas of consensus, unmet needs and opportunities for further study. *Hepatology*. 2019;69(5):2271–2283.
3. Crabb DW, Im GY, Szabo G, Mellinger JL, Lucey MR. Diagnosis and treatment of alcohol-associated liver diseases: 2019 practice guidance from the American Association for the Study of Liver Diseases. *Hepatology*. 2020;71(1):306–333.
4. Bertola A, Mathews S, Ki SH, Wang H, Gao B. Mouse model of chronic and binge ethanol feeding (the NIAAA model). *Nat Protoc*. 2013;8(3):627–637.
5. Lazaro R, et al. Osteopontin deficiency does not prevent but promotes alcoholic neutrophilic hepatitis in mice. *Hepatology*. 2015;61(1):129–140.
6. Chao X, et al. Impaired TFEB-mediated lysosome biogenesis and autophagy promote chronic ethanol-induced liver injury and steatosis in mice. *Gastroenterology*. 2018;155(3):865–879.e12.
7. Sanz-Garcia C, et al. The non-transcriptional activity of IRF3 modulates hepatic immune cell populations in acute-on-chronic ethanol administration in mice. *J Hepatol*. 2019;70(5):974–984.
8. Cai Y, et al. Mitochondrial DNA-enriched microparticles promote acute-on-chronic alcoholic neutrophilia and hepatotoxicity. *JCI Insight*. 2017;2(14):e92634.
9. Thurman RG, et al. The role of gut-derived bacterial toxins and free radicals in alcohol-induced liver injury. *J Gastroenterol Hepatol*. 1998;13(S1):S39–S50.
10. Tsukamoto H, Lu SC. Current concepts in the pathogenesis of alcoholic liver injury. *FASEB J*. 2001;15(8):1335–1349.
11. Hoek JB, Cahill A, Pastorino JG. Alcohol and mitochondria: a dysfunctional relationship. *Gastroenterology*. 2002;122(7):2049–2063.
12. Arteel G, Marsano L, Mendez C, Bentley F, McClain CJ. Advances in alcoholic liver disease. *Best Pract Res Clin Gastroenterol*. 2003;17(4):625–647.
13. Guyton KZ, Liu Y, Gorospe M, Xu Q, Holbrook NJ. Activation of mitogen-activated protein kinase by H2O2. Role in cell survival following oxidant injury. *J Biol Chem*. 1996;271(8):4138–4142.
14. Nagai H, Noguchi T, Takeda K, Ichijo H. Pathophysiological roles of ASK1-MAP kinase signaling pathways. *J Biochem Mol Biol*. 2007;40(1):1–6.
15. Kamata H, Honda S, Maeda S, Chang L, Hirata H, Karin M. Reactive oxygen species promote TNFalpha-induced death and sustained JNK activation by inhibiting MAP kinase phosphatases. *Cell*. 2005;120(5):649–661.
16. Matsuzawa A, Ichijo H. Redox control of cell fate by MAP kinase: physiological roles of ASK1-MAP kinase pathway in stress signaling. *Biochim Biophys Acta*. 2008;1780(11):1325–1336.
17. Kim DH, et al. A conserved p38 MAP kinase pathway in Caenorhabditis elegans innate immunity. *Science*. 2002;297(5581):623–626.
18. Zarubin T, Han J. Activation and signaling of the p38 MAP kinase pathway. *Cell Res*. 2005;15(1):11–18.
19. Cuenda A, Rousseau S. p38 MAP-kinases pathway regulation, function and role in human diseases. *Biochim Biophys Acta*. 2007;1773(8):1358–1375.
20. Wagner EF, Nebreda AR. Signal integration by JNK and p38 MAPK pathways in cancer development. *Nat Rev Cancer*. 2009;9(8):537–549.
21. Song Z, Wang Y, Zhang F, Yao F, Sun C. Calcium signaling pathways: key pathways in the regulation of obesity. *Int J Mol Sci*. 2019;20(11):E2768.
22. Wang Y, et al. Hepatocyte tnf receptor-associated factor 6 aggravates hepatic inflammation and fibrosis by promoting lysine 6-linked polyubiquitination of apoptosis signal-regulating kinase 1. *Hepatology*. 2020;71(1):93–111.
23. Yan ZZ, et al. Integrated omics reveals tollip as an regulator and therapeutic target for hepatic ischemia-reperfusion injury in mice. *Hepatology*. 2019;70(5):1750–1769.
24. Huang Z, et al. Dual specificity phosphatase 12 regulates hepatic lipid metabolism through inhibition of the lipogenesis and apoptosis signal-regulating kinase 1 pathways. *Hepatology*. 2019;70(4):1099–1118.
25. Hwang S, et al. Interleukin-22 ameliorates neutrophil-driven nonalcoholic steatohepatitis through multiple targets [published ahead of print November 9, 2019]. *Hepatology*. doi: 10.1002/hep.31031.
26. Zhang X, et al. Macrophage p38α promotes nutritional steatohepatitis through M1 polarization. *J Hepatol*. 2019;71(1):163–174.
27. Xu MJ, et al. Fat-specific protein 27/CIDEC promotes development of alcoholic steatohepatitis in mice and humans. *Gastroenterology*. 2015;149(4):1030–1041.e6.
28. Tobiume K, et al. ASK1 is required for sustained activations of JNK/p38 MAP kinases and apoptosis. *EMBO Rep*. 2001;2(3):222–228.
29. Saitoh M, et al. Mammalian thioredoxin is a direct inhibitor of apoptosis signal-regulating kinase (ASK) 1. *EMBO J*.

1998;17(9):2596–2606.
30. Raposo G, Stoorvogel W. Extracellular vesicles: exosomes, microvesicles, and friends. *J Cell Biol*. 2013;200(4):373–383.
31. Gurunathan S, Kang MH, Jeyaraj M, Qasim M, Kim JH. Review of the isolation, characterization, biological function, and multifarious therapeutic approaches of exosomes. *Cells*. 2019;8(4):E307.
32. Trajkovic K, et al. Ceramide triggers budding of exosome vesicles into multivesicular endosomes. *Science*. 2008;319(5867):1244–1247.
33. Lang JK, Young RF, Ashraf H, Canty JM. Inhibiting extracellular vesicle release from human cardiosphere derived cells with lentiviral knockdown of nSMase2 differentially effects proliferation and apoptosis in cardiomyocytes, fibroblasts and endothelial cells in vitro. *PLoS One*. 2016;11(11):e0165926.
34. Blanc L, Vidal M. New insights into the function of Rab GTPases in the context of exosomal secretion. *Small GTPases*. 2018;9(1–2):95–106.
35. Ostrowski M, et al. Rab27a and Rab27b control different steps of the exosome secretion pathway. *Nat Cell Biol*. 2010;12(1):19–30.
36. Thornalley PJ, Vasák M. Possible role for metallothionein in protection against radiation-induced oxidative stress. Kinetics and mechanism of its reaction with superoxide and hydroxyl radicals. *Biochim Biophys Acta*. 1985;827(1):36–44.
37. Zhou Z, Sun X, Lambert JC, Saari JT, Kang YJ. Metallothionein-independent zinc protection from alcoholic liver injury. *Am J Pathol*. 2002;160(6):2267–2274.
38. Zhou Z, Sun X, James Kang Y. Metallothionein protection against alcoholic liver injury through inhibition of oxidative stress. *Exp Biol Med (Maywood)*. 2002;227(3):214–222.
39. Cargnello M, Roux PP. Activation and function of the MAPKs and their substrates, the MAPK-activated protein kinases. *Microbiol Mol Biol Rev*. 2011;75(1):50–83.
40. Mathurin P, et al. Selonsertib in combination with prednisolone for the treatment of severe alcoholic hepatitis: a phase 2 randomized controlled trial. *Hepatology*. 2018;68:8A–9A.
41. Schuster-Gaul S, et al. ASK1 inhibition reduces cell death and hepatic fibrosis in an Nlrp3 mutant liver injury model. *JCI Insight*. 2020;5(2):e123294.
42. Cuadrado A, Nebreda AR. Mechanisms and functions of p38 MAPK signalling. *Biochem J*. 2010;429(3):403–417.
43. Enslen H, Raingeaud J, Davis RJ. Selective activation of p38 mitogen-activated protein (MAP) kinase isoforms by the MAP kinase kinases MKK3 and MKK6. *J Biol Chem*. 1998;273(3):1741–1748.
44. Jiang Y, et al. Characterization of the structure and function of a new mitogen-activated protein kinase (p38beta). *J Biol Chem*. 1996;271(30):17920–17926.
45. Stein B, et al. p38-2, a novel mitogen-activated protein kinase with distinct properties. *J Biol Chem*. 1997;272(31):19509–19517.
46. Mertens S, Craxton M, Goedert M. SAP kinase-3, a new member of the family of mammalian stress-activated protein kinases. *FEBS Lett*. 1996;383(3):273–276.
47. Goedert M, Cuenda A, Craxton M, Jakes R, Cohen P. Activation of the novel stress-activated protein kinase SAPK4 by cytokines and cellular stresses is mediated by SKK3 (MKK6); comparison of its substrate specificity with that of other SAP kinases. *EMBO J*. 1997;16(12):3563–3571.
48. Jiang Y, et al. Characterization of the structure and function of the fourth member of p38 group mitogen-activated protein kinases, p38delta. *J Biol Chem*. 1997;272(48):30122–30128.
49. Hwang S, et al. Protective and detrimental roles of p38α MAPK in different stages of nonalcoholic fatty liver disease [published ahead of print May 28, 2020]. *Hepatology*. https://doi.org/10.1002/hep.31390.
50. Wang X, et al. Cyclophilin D deficiency attenuates mitochondrial perturbation and ameliorates hepatic steatosis. *Hepatology*. 2018;68(1):62–77.
51. Curtis AM, Wilkinson PF, Gui M, Gales TL, Hu E, Edelberg JM. p38 mitogen-activated protein kinase targets the production of proinflammatory endothelial microparticles. *J Thromb Haemost*. 2009;7(4):701–709.
52. Verderio C, Gabrielli M, Giussani P. Role of sphingolipids in the biogenesis and biological activity of extracellular vesicles. *J Lipid Res*. 2018;59(8):1325–1340.
53. Li J, et al. Microvesicles shed from microglia activated by the P2X7-p38 pathway are involved in neuropathic pain induced by spinal nerve ligation in rats. *Purinergic Signal*. 2017;13(1):13–26.
54. Garcia-Martinez I, et al. Hepatocyte mitochondrial DNA drives nonalcoholic steatohepatitis by activation of TLR9. *J Clin Invest*. 2016;126(3):859–864.
55. Shimada K, et al. Oxidized mitochondrial DNA activates the NLRP3 inflammasome during apoptosis. *Immunity*. 2012;36(3):401–414.
56. Itagaki K, et al. Mitochondrial DNA released by trauma induces neutrophil extracellular traps. *PLoS One*. 2015;10(3):e0120549.
57. Yousefi S, Mihalache C, Kozlowski E, Schmid I, Simon HU. Viable neutrophils release mitochondrial DNA to form neutrophil extracellular traps. *Cell Death Differ*. 2009;16(11):1438–1444.
58. Lood C, et al. Neutrophil extracellular traps enriched in oxidized mitochondrial DNA are interferogenic and contribute to lupus-like disease. *Nat Med*. 2016;22(2):146–153.
59. Tobiume K, et al. ASK1 is required for sustained activations of JNK/p38 MAP kinases and apoptosis. *EMBO Rep*. 2001;2(3):222–228.
60. Kim SJ, et al. Adipocyte death preferentially induces liver injury and inflammation through the activation of chemokine (C-C motif) receptor 2-positive macrophages and lipolysis. *Hepatology*. 2019;69(5):1965–1982.
61. He Y, et al. MicroRNA-223 ameliorates nonalcoholic steatohepatitis and cancer by targeting multiple inflammatory and oncogenic genes in hepatocytes. *Hepatology*. 2019;70(4):1150–1167.
62. Seo W, et al. ALDH2 deficiency promotes alcohol-associated liver cancer by activating oncogenic pathways via oxidized DNA-enriched extracellular vesicles. *J Hepatol*. 2019;71(5):1000–1011.